ELSEVIER

Physica C 312 (1999) 225–232

PHYSICA C

Ba–Ca–Cu oxycarbonate thin films, prepared by pulsed laser deposition: structure, growth mechanism and superconducting properties

G. Calestani [a,b], A. Migliori [a], U. Spreitzer [c], S. Hauser [c], M. Fuchs [c], H. Barowski [c], T. Schauer [c], W. Assmann [d], K.-J. Range [e], A. Varlashkin [c,1], O. Waldmann [f], P. Müller [f], K.F. Renk [c,*]

[a] *CNR-LAMEL, Area della Ricerca di Bologna, I-40129 Bologna, Italy*
[b] *Dipartimento di Chimica Generale ed Inorganica, Chimica Fisica e Chimica Analitica, Università di Parma, I-43100 Parma, Italy*
[c] *Institut für Experimentelle und Angewandte Physik, Universität Regensburg, D-93040 Regensburg, Germany*
[d] *Institut für Experimentelle Kernphysik und Beschleunigerlaboratorium, Sektion Physik der LMU, München, D-85748 Garching, Germany*
[e] *Institut für Anorganische Chemie, Universität Regensburg, D-93040 Regensburg, Germany*
[f] *Institut für Physik III, Universität Erlangen-Nürnberg, Erwin Rommel-Str. 1, D-91058 Erlangen, Nürnberg, Germany*

Received 14 September 1998; revised 27 November 1998; accepted 3 December 1998

Abstract

Ba–Ca–Cu oxycarbonate superconducting thin films on $LaAlO_3$ (100) substrates were grown by pulsed laser deposition in off axis geometry. X-ray diffraction, selected area electron diffraction, and high-resolution transmission electron microscopy indicated that the films consisted of different phases of the $(C_xCu_{1-x})Ba_2Ca_{n-1}Cu_nO_{2n+3}$ compound. The main phase was the $n=4$ phase $(C_xCu_{1-x})Ba_2Ca_3Cu_4O_{11}$, besides other phases as the $n=1,2,3,5\ldots$ phases and precipitates of CaO. The films were grown predominantly *a*-axis oriented and contained, in a small amount, *c*-axis oriented domains of the $n=4$ phase near the film surface. An onset of superconductivity at 115 K and critical temperatures up to 78 K were found by AC resistive and inductive measurements.

PACS: 74.Fq 74.76.Bz; 61.16.Bg
Keywords: Superconducting films; Transmission and scanning electron microscopy; Ba–Ca–Cu oxycarbonate

1. Introduction

During the last years, several groups reported on Ba–Ca–Cu oxycarbonate superconductors [1–5]. The structure of these compounds consists of $CaCuO_2$ infinite layer blocks separated by charge carrier blocks containing CO_3 groups, either sandwiched, or alone, or in combination with CuO_x groups between Ba layers. The compounds can be represented by the general chemical formula $(C_xCu_{1-x})_mBa_{m+1}Ca_{n-1}Cu_nO_{2n+m+2}$ with $n=1,2,3,4\ldots$. Except for the most simple compound ($m=1$ and $n=1$), the preparation requires special conditions. $(C_xCu_{1-x})Ba_2Ca_{n-1}Cu_nO_{2n+3}$ with $n=2,3,4\ldots$ has been

* Corresponding author. Tel.: +49-941-943-2074; Fax: +49-941-943-4223; E-mail: karl.renk@physik.uni-regensburg

[1] Present address: Lebedev Physics Institute of the Academy of Sciences, Leninskii Prospect 53, 117924 Moscow, Russian Federation.

0921-4534/99/$ - see front matter
PII: S0921-4534(98)00681-9

prepared by high-pressure synthesis with the samples being characterized by 1:1 mixed Cu:C layers. Among these oxycarbonates, the $n = 4$ phase $(C_{0.5}Cu_{0.5})Ba_2Ca_3Cu_4O_{11}$, abbreviated as $(C_{0.5}Cu_{0.5})$-1234, which shows a T_c of 117 K, is of special interest, because its irreversibility field B_{IRR} at 77 K is higher than that of Bi-2212 or Hg-1223 [6].

Recently, the preparation of thin films of Ba–Ca–Cu oxycarbonates by pulsed laser deposition [7–10] and sputtering [11,12] has been reported. The films prepared by pulsed laser deposition showed a simultaneous intergrowth of $(CaCuO_2)_p$ and $(Ba_2CuO_2CO_3)_q$ structural blocks and the main phase was that with $p = 3$ and $q = 1$. This phase, with almost complete CO_3 layers [7], is structurally similar to the $(C_{0.5}Cu_{0.5})$-1234 phase, which has, however, mixed Cu:C layers. The films showed critical temperatures up to 75 K and a semiconductor-like behavior of the resistivity above the critical temperature. The films were grown *a*-axis oriented, i.e., with the stacking axis *c* parallel to the substrate.

In this paper, the preparation of superconducting thin films of Ba–Ca–Cu oxycarbonate by pulsed laser deposition is reported, together with a detailed characterization of the films by several techniques. We used pulsed laser deposition in off axis geometry, where the substrate is perpendicular to the target surface [13,14]. With this geometry, different parameters (e.g., substrate temperature and laser beam energy), which are relevant for the film growth, can be varied almost independently [13]. This is of importance under the viewpoint that, as mentioned by Allen et al. [7], the range of parameters suitable for deposition of Ba–Ca–Cu oxycarbonate thin films is very small. We have investigated the film structure using different techniques, namely X-ray diffraction (XRD), selected area electron diffraction analysis (SAED), high resolution electron microscopy (HREM), energy dispersion X-ray analysis (EDX), and furthermore, elastic recoil detection analysis (ERDA) [15]. We studied, for the first time, Ba–Ca–Cu oxycarbonate films by HREM investigations taken on cross-section. These investigations allowed us to determine the film structure from regions at the film–substrate interface up to first nanometers of the film and, thus, on the mechanism of film growth.

2. Experimental

The films were prepared by pulsed laser deposition in off axis geometry [13,14]. The beam of a KrF excimer laser (wavelength = 248 nm, fluence = 4 J/cm^2, pulse duration = 15 ns, repetition rate = 10 Hz) was directed through an Al_2O_3 ceramic tube (length = 4 cm, inner diameter = 25 mm) containing a heating element (FeAlCr). The substrate was mounted inside the tube on a rotating substrate holder. The distance between target and substrate was about 35 mm. The substrate holder covered three of the four gable-ends and five small areas on each surface side.

The target was prepared by a citrate gel process [16,17]. Oxide powders of Ba, Ca, and Cu in a ratio Ba:Ca:Cu:O as 2:3:5:10 (5 g, 6×10^{-3} mole of $Ba_2Ca_3Cu_5O_{10}$) were mixed and dissolved in bidestillated water and HNO_3. After heating (to about 100°C), 100 ml of an aqueous solution of citric acid (CA) and ethylene glycol (EG) (62.5 ml H_2O, 6.4×10^{-2} mole CA and 2.56×10^{-1} mole EG) in a ratio of 1:4 was added and heated (to about 140°C). The gel was pyrolysed at 450°C for 10 h under flowing oxygen, the resulting ash was deposited in an aluminia crucible and heated for 32 h at 835°C under flowing oxygen. Then the powder was pressed into pellets at a pressure of 3×10^8 Pa and annealed again under flowing oxygen at 940°C for 7 h. XRD investigations (Θ–2Θ-scan) showed, that the target contained the compounds $BaCuO_2$, Ca_2CuO_3, Cu, and in a small amount, CaO and CuO. X-ray photoemission spectrometry (XPS) indicated that the C content was below the limit of detection (1 at.%), while on the surface of the target (up to several nanometers), the C content reached concentrations up to 30 at.%. Most likely, the target absorbed CO_2 from the laboratory atmosphere during opening of the chamber; we opened the chamber for grinding the target surface or changing the substrate.

During ablation, with a substrate at 645°C in an atmosphere containing CO_2 (9%) and O_2 at a total pressure of 0.4 mbar, the pressure decreased slightly (to 0.36 mbar), because ablated material from the target, which was deposited on the heater surface, absorbed O_2 and particularly CO_2. After deposition, the oxygen partial pressure was increased to 700 mbar and the film was cooled to room temperature

(at a rate of 35°C/min). Below 250°C, the cooling rate decreased according to the large amount of thermal energy stored in the heating tube. $LaAlO_3$ (100) was used as substrate, because its lattice period ($a = 0.379$ nm) is close to that along the *a*-axis of the tetragonal $(C_{0.5}Cu_{0.5})$-1234 structure ($a = 0.385$ nm) [1–4].

An XRD analysis was performed with a Philips PW1050 powder diffractometer using Ni-filtered Cu K_α radiation. TEM investigations were performed with a Philips CM30 microscope operating at 300 kV. The samples were prepared both in planar and in cross-sections by mechanical polishing and ion beam thinning using argon atoms accelerated to 5 keV. The ERDA measurements were made with 10 MeV ions at a scattering angle of 37.6°.

The superconducting properties of a Ba–Ca–Cu oxycarbonate film were characterized by an AC inductive (10 kHz, 10^{-6} T, *B* field perpendicular to the film surface) and an AC resistive measurement with a four-point technique (1 kHz, 10^{-7} A). The surface resistance was measured at 86 GHz using a cylindrical copper cavity (diameter = 8.1 mm) on which the Ba–Ca–Cu oxycarbonate film was mounted as endplate. The power of the radiation (TE_{021} mode) was 10 mW providing peak magnetic fields of about 20 A/m at the surface of the superconducting sample [18]. DC magnetization measurements (zero field cooling, ZFC, and field cooling, FC, magnetic field *B* of 1 or 10 G perpendicular and parallel to the film surface) were performed with a SQUID magnetometer (Quantum Design).

3. Results and discussion

3.1. Structural and microstructural characterization

Under our typical deposition conditions, the film growth rate was 50 nm/min. The film surfaces were black and mirror-like. At the edges of a film surface (substrate size = 10 × 10 × 1 mm), the film had a lower T_c, in comparison to the center, or was even not superconducting; this was caused by a too strong heating of the edges during the growth process. The overall chemical composition of the Ba–Ca–Cu oxycarbonate thin films as well as a possible variation of the composition of single species during the deposition process was studied by ERDA and EDX. Fig. 1 shows the depth profile of the Ba–Ca–Cu oxycarbonate thin film. Accordingly, there was an almost homogenous distribution of C:Ca:Cu:O throughout the film. The overall composition of the film from ERDA and EDX was C:Ba:Ca:Cu:O as 0.7:1.8:4.6:4.5:13.5.

Structural and microstructural characterizations were performed by combining XRD, SAED, and HREM. TEM investigations revealed that the films showed a particular microstructure, namely a columnar microstructure perpendicular to the substrate. This is shown in Fig. 2a for one of our films. The microstructure extended up to the film surface. The columns had a typical section of about 100 nm and were separated to a large extent by voids, which increased from the substrate toward the film surface. From the TEM image of a plane section of a film (Fig. 2b), the columns appear to consist of grains in which the stacking axis *c* of the oxycarbonate layered structure was parallel to the section, randomly distributed in two orientations which were tilted by 90°.

The XRD pattern (Fig. 3) was complex and a complete assignment of the diffraction peaks was made possible by the knowledge of the results of the HREM study. The patterns were dominated, depending on the film thickness, by the *h*00 reflections of both the $LaAlO_3$ substrate and the tetragonal $(C_xCu_{1-x})Ba_2Ca_{n-1}Cu_nO_{2n+3}$ structure, indicating that the films grew with the *a*-axis perpendicular to the substrate, in agreement with the TEM observation. This is at first sight surprising, since according

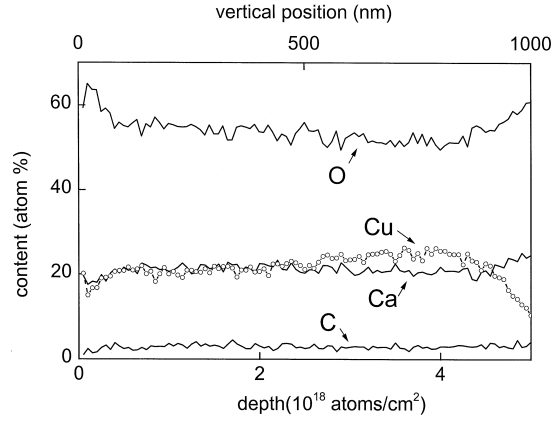

Fig. 1. ERDA pattern of a Ba–Ca–Cu oxycarbonate thin film.

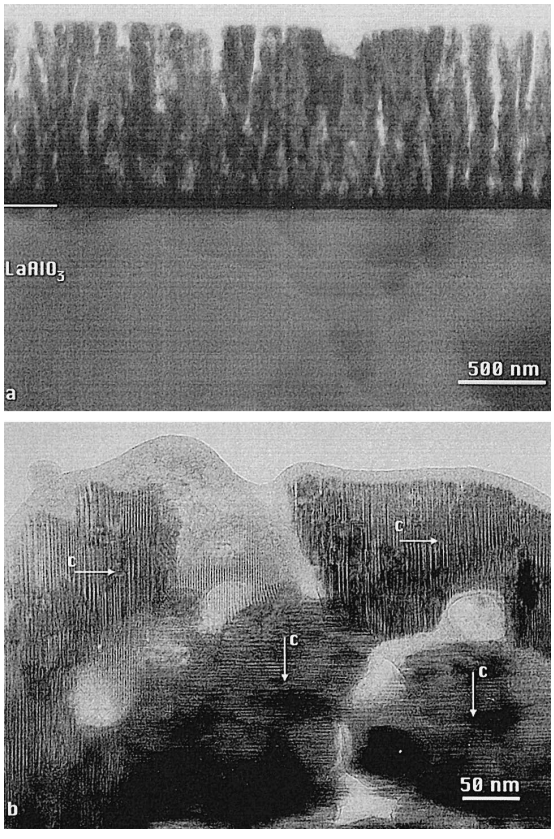

Fig. 2. TEM images of both cross (a) and planar (b) sections of the Ba–Ca–Cu oxycarbonate thin film.

to the similarity of the lattice parameters, the film was expected to grow epitaxially with the *c*-axis perpendicular to the substrate. However, a series of weaker reflections, which can be indexed as a $00l$ sequence related to a periodicity of 1.825 nm, may indicate that a minor part of the film, consisting of the (C_xCu_{1-x})-1234 phase, was grown *c*-axis oriented, i.e., with the *c*-axis perpendicular to the substrate surface. Moreover, the XRD pattern showed isolated reflection sets, indicating the presence of further epitaxially grown phases, with isolated sets of reflections. In particular, a single peak corresponding to a period of 0.240 nm suggests the presence of CaO, whereas a sequence with a period of 0.404 nm can be related to the barium copper oxycarbonate $(C_{1-x}Cu_x)BaCuO_5$. This compound represents the simplest member $(n=1)$ of the $(C_xCu_{1-x})Ba_2Ca_{n-1}Cu_nO_{2n+3}$ homologous series and can be stabilized by partial substitution of Ca for Cu in the CuO_2 layers. Depending on the relative C, Cu, and Ca concentrations, it presents several perovskite-related superstructures, which are characterized, with respect to the other member of the series, by an increased basal periodicity [19].

More information was obtained by electron diffraction. Fig. 4 shows a typical SAED of a cross-

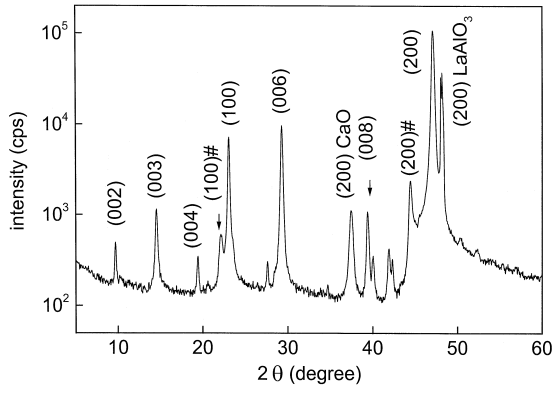

Fig. 3. XRD pattern of a Ba–Ca–Cu oxycarbonate thin film. The symbol '#' indicates the $(C_{1-x}Cu_x)BaCuO_5$ compound.

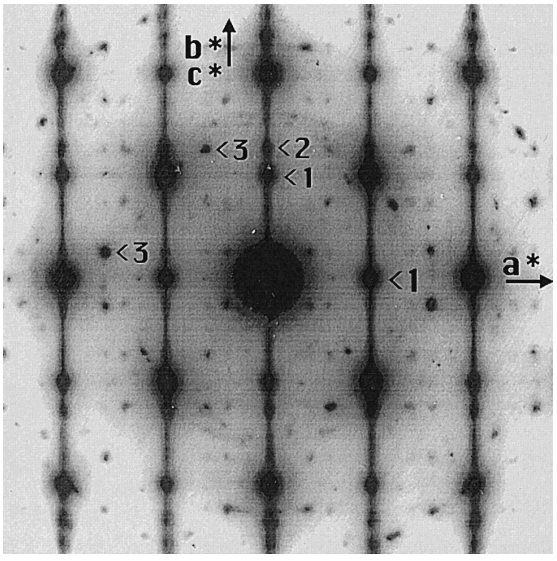

Fig. 4. SAED pattern taken on a cross-section. The spot labeled (1) corresponds to (100) or (010) Ba–Ca–Cu oxycarbonate reflections, while the spot (2) corresponds to (006) reflection of the $n=4$ phase. The spot (3) arises from (111) planes of CaO precipitates; these spots are repeated by double reflections around the $h0l$ and $hk0$ spots of the Ba–Ca–Cu oxycarbonate, indicating an epitaxial growth of CaO domains.

section of a Ba–Ca–Cu oxycarbonate thin film. The pattern can be explained by supposing the simultaneous presence of $h0l$ and $hk0$ reflections of the Ba–Ca–Cu oxycarbonate, originated by a domain structure in which the *a*-axis, perpendicular to the substrate surface, is preserved and twinned domains are mutually tilted by 90° in the *bc* plane (Fig. 2b). The streaking observed along the $c*$-axis, typically produced by disordered stacking of structural blocks with different periodicity, indicates a structural inhomogeneity of the deposited material, consisting of intercalation of different $(C_xCu_{1-x})Ba_2Ca_{n-1}Cu_nO_{2n+3}$ phases. However, since discrete contributions are observed along $c*$ only for d values in agreement with those expected for the (C_xCu_{1-x})-1234 phase, the $n=4$ phase seems to be the only phase which gave rise to structural sequences ordered on a range greater than the coherence length of the electron beam. As in case of the XRD pattern, the SAED pattern (Fig. 4) shows reflections, which can be attributed to CaO. Primary (111) and (200) reflections of two domains of CaO, which are slightly shifted in an equivalent way from the [110] pole, are visible in Fig. 4. The spots are repeated by double reflection around $h0l$ and $hk0$ spots of the Ba–Ca–Cu oxycarbonate, indicating an epitaxial growth of CaO domains.

HREM characterization, performed mostly on cross-section of the superconducting Ba–Ca–Cu oxycarbonate thin films, showed that the samples consisted mainly of disordered stacking of structural blocks with different periodicity, as evidenced by the streaking observed along $c*$ in the SAED patterns. Examples are shown in Fig. 5, where different numbers of CuO_2 layers intercalated between the BaO–(C_xCu_{1-x})–BaO blocks, corresponding to the different phases of the $(C_xCu_{1-x})Ba_2Ca_{n-1}Cu_nO_{2n+3}$ structure, are indicated on the images. From the HREM study, the main phase is the $n=4$ phase. The probability to find other phases decreased with rising n for $n>4$ and also with decreasing n for $n<4$. However, the distribution of the different phases depended critically on the distance from the substrate. This allowed to develop a hypothesis on the mechanism of the film growth.

At the interface with the substrate, a film consisted mainly of the simple $n=1$ and $n=2$ phases, with the *c*-axis parallel to the substrate surface.

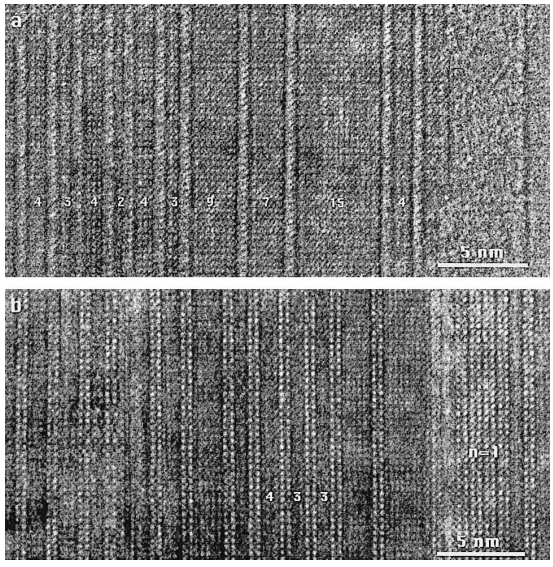

Fig. 5. HREM images taken on a cross-section of a superconducting Ba–Ca–Cu oxycarbonate thin film, near the surface (a) and in the central region (b), showing intercalations of different phases along *c*. The number of CuO_2 layers intercalated between the BaO–(C_xCu_{1-x})–BaO blocks are indicated. Due to different experimental parameters (defocus and sample thickness), the barium atoms are represented in (a) by black fringes and in (b) by bright spots.

These influenced the further film growth. The region is characterized by frequent 90° microtwinning in the *bc* plane of the film and by segregation of CaO islands (Fig. 6). The superimposition of different phases or of differently oriented grains makes the HREM study of the growth at the substrate–film interface difficult, since the contrast is reduced and Moiré interference fringes are produced. The best match between substrate and film was observed for ordered domains of the $n=2$ phases. This can be justified by the quite good superposition of the *c*-axis of the $n=2$ oxycarbonate with three substrate cells (≈ 1.14 nm), as can be observed in Fig. 7. The growth of the $n=1$ phase at the interface may be favored by the possibility of this phase to modulate, in particular, by varying the carbon and copper content, the *c* lattice parameter to match the substrate. In both cases, the structural matching requires the *c*-axis of the oxycarbonate to be in the plane of the substrate and therefore it forces an *a*-oriented growth.

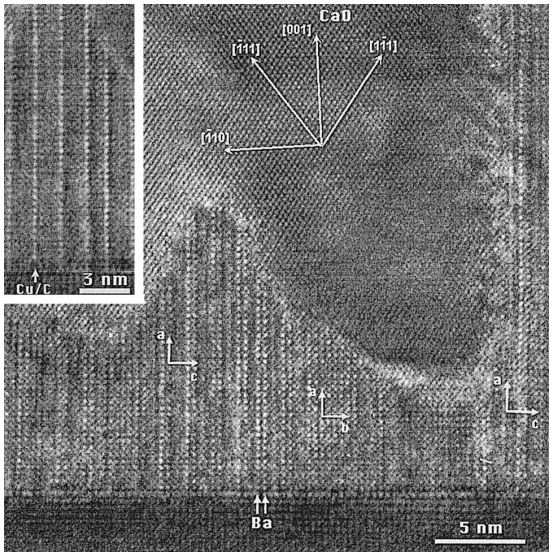

Fig. 6. HREM image taken on a cross-section at the film–substrate interface at a defocus of about 100 nm. Frequent microtwinnnig in the *bc* plane of the film (some are indicated) are visible, as well as the segregation of a large CaO precipitate. In the central region, where Ba rows are indicated by arrows, an *n* sequence 3-3-3-2-3 is recognizable. The same region, taken at a Scherzer defocus ($\Delta f = -77$) evidencing as bright rows the Cu/C layers, is shown in the inset. The mutual orientation of film and precipitate is indicated.

The growth at the interface of phases that are Ba- and Cu-rich, with respect to the ablated material, results in the segregation of CaO precipitates. Different precipitates have been studied by HREM and it was found, in agreement with XRD and SAED results, that CaO grows epitaxially on the Ba–Ca–Cu oxycarbonate as shown in Fig. 6. The CaO precipitates were, during the film growth, at the origin of the formation of voids among the oxycarbonate columns. In fact, with increasing film thickness, the number of CuO_2 layers intercalated between the BaO–(C_xCu_{1-x})–BaO blocks, increased to values which were, in the average, compatible with the composition of the ablated material. The segregation of CaO was stopped, but the growth continued preferentially on the existing oxycarbonate, so that intercolumnar voids were produced.

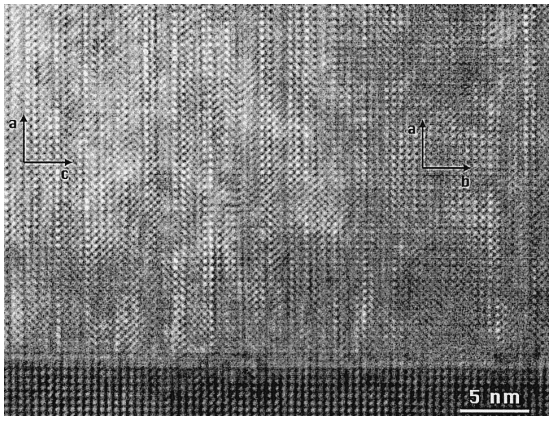

Fig. 7. HREM image taken on a cross-section at the film–substrate interface. An *ac*-oriented domain with an almost ordered $n = 2$ sequence and some $n = 1$ intercalation is shown on the left, whereas a smaller *ab*-oriented domain is shown on the right. Brighter spots represent Ba atoms. A good structural match with the substrate is obtained for the *ac* domain.

In contrast to the XRD analysis, no evidence of *c*-oriented domains was found by HREM. The 00*l* diffraction sequence of the $n = 4$ phases, observed in XRD, could have been produced by isolated island on (or near) the film surface, which have been damaged or destroyed during the preparation of the sample for the TEM characterization. During this process, the film surface has been, in a first step, covered with glue, which has been removed by the ion beam at least in the area suitable for the HREM investigation.

3.2. Electrical and magnetic properties

AC resistive measurements showed (Fig. 8) a strong reduction of the resistivity between 115 K and

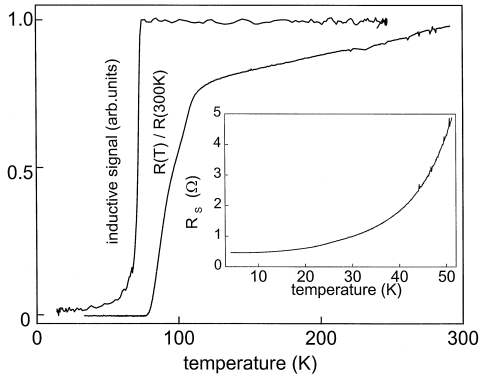

Fig. 8. AC mutual inductive and AC resistive measurements of a Ba–Ca–Cu oxycarbonate thin film showing a critical temperature of 74 K (inductive) and 78 K (resistive). Inset: surface resistance R_S (at 86 GHz) of a superconducting Ba–Ca–Cu oxycarbonate thin film.

the critical temperature (78 K). Above 115 K, the film showed a metal-like temperature behavior. The specific resistivity at 300 K (3×10^{-4} Ω m) was about two orders of magnitude higher than of other epitaxial grown high-T_c films (e.g., YBCO films). Extrapolation of the resistivity down to 0 K resulted in a residual resistivity of $0.7R$(300 K). The high residual resistivity indicates, that the film contained many grain boundaries, as seen from HREM investigations. The magnetic shielding showed a critical temperature of 74 K (Fig. 8). The complete screening indicates, that there were shielding currents on an area with a diameter of several millimeters.

The surface resistance (at 86 GHz) showed a reduction from 5 Ω at 50 K to 0.5 Ω at 4.2 K (Fig. 8, insert). The high values of R_S (especially at 4.2 K) were caused by holes, grain edges (weak links), and nonsuperconducting parts.

We performed a DC magnetization measurement with the magnetic field ($B = 10$ G) parallel and perpendicular to the film surface (Fig. 9). For the magnetic field parallel to the film surface, the ZFC curve showed a diamagnetic signal (onset near 60 K) indicating a magnetic moment of -1×10^{-5} emu at 5 K. The FC curve showed no diamagnetic signal. For the magnetic field perpendicular to the film surface, the ZFC and the FC curve showed diamagnetic signals (onset at 62 K) according to a magnetic moment of -9×10^{-6} emu (ZFC, at 5 K) and -4×10^{-4} emu (FC, at 5 K). The difference in the critical temperature and in the diamagnetic moment between the measurements with B parallel and perpendicular to the film surface may be caused by the film morphology. Because of the voids, there were more paths for shielding currents parallel than perpendicular to the film surface.

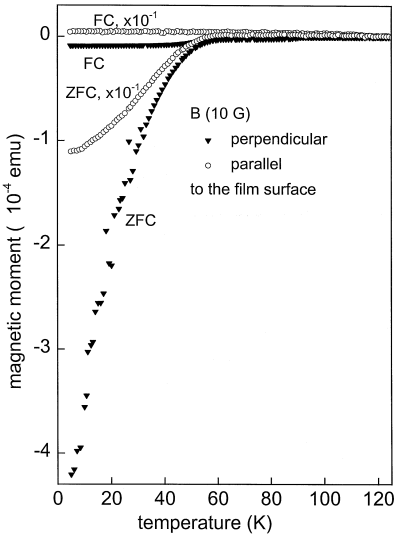

Fig. 9. DC magnetic measurement of a Ba–Ca–Cu oxycarbonate thin film made with a SQUID magnetometer. Magnetic field of 10 G applied parallel and perpendicular to the film surface.

There was a difference of the critical temperatures of 62 K (DC measurement) and 74 K (AC measurement) for the same film most likely because the DC measurements were made several months after the film preparation, while the AC measurement has been made for the fresh film.

The results of the electric and magnetic properties indicate superconductivity in small areas (at least several unit cells) at temperatures of about 115 K, which is consistent with different phases of the Ba–Ca–Cu oxycarbonate having different critical temperatures.

4. Conclusion

In summary, we have studied superconducting films of Ba–Ca–Cu oxycarbonate superconductors prepared by pulsed laser deposition on $LaAlO_3$ (100) substrates. The films contained as main phase the (C_xCu_{1-x})-1234 phase. The results indicate the possibility of preparation of thin (C_xCu_{1-x})-1234 films with similar properties (e.g., T_c of 115 K) as obtained for samples prepared by high-pressure synthesis [1–5].

Acknowledgements

We would like to thank Th. Kaiser (Bergische Universität-GH Wuppertal) for the HF measurements, D. Schepp (Universität Regensburg) for EDX measurements and J. Vancea (Universität Regensburg) for XPS measurements. Support by the Bayerische Forschungsstiftung through the Bayerischer Forschungsverbund Hochtemperatur-Supraleiter (FORSUPRA) is acknowledged.

References

[1] T. Kawashima, Y. Matsui, E. Takayama-Muromachi, Physica C 224 (1994) 69.
[2] T. Kawashima, Y. Matsui, E. Takayama-Muromachi, Physica C 227 (1994) 95.
[3] T. Kawashima, Y. Matsui, E. Takayama-Muromachi, Physica C 233 (1994) 143.
[4] Y. Matsui, T. Kawashima, E. Takayama-Muromachi, Physica C 235–240 (1994) 166.
[5] M.A. Alario-Franco, P. Bordet, J.J. Capponi, C. Chaillout, J. Chenavas, T. Fournier, M. Marezio, B. Souletie, A. Sulcipe, J.-L. Tholence, C. Colliex, R. Argoud, J.L. Baldonedo, M.F. Gorius, M. Perroux, Physica C 231 (1994) 103.
[6] H. Kumakura, H. Kitaguchi, K. Togano, T. Kawashima, E. Takayama-Muromachi, S. Okayasu, Y. Kazumata, IEEE Trans. Appl. Supercond. 5 (2) (1993) 1399.
[7] L. Allen, B. Mercey, W. Prellier, J.F. Hamet, M. Hervieu, B. Raveau, Physica C 241 (1995) 158.
[8] W. Prellier, J.L. Allen, C. Prouteau, Ch. Simon, B. Mercey, Supercond. Sci. Technol. 8 (1995) 361.
[9] B. Raveau, C. Michel, B. Mercey, J.F. Hamet, M. Hervieu, Journal of Alloys and Compounds 229 (1995) 134.
[10] B. Raveau, C. Michel, M. Hervieu, C.R. Acad. Sci. Paris 322 (1996) 609, Series II b.
[11] M. Sakai, K. Mizuno, H. Adachi, K. Setsune, in: K. Yamafuki, T. Morishita (Eds.), Advances in Superconductivity VII, Springer, Tokyo, 1995, pp. 397–400.
[12] H. Adachi, M. Sakai, T. Satoh, K. Setsune, in: H. Hayakama, Y. Enomoto (Eds.), Advances in Superconductivity VIII, Springer, Tokyo, 1995, pp. 955–960.
[13] B. Holzapfel, B. Roas, L. Schultz, P. Bauer, G. Saemann-Ischenko, Appl. Phys. Lett. 61 (1992) 3178.
[14] N. Reschauer, U. Spreitzer, W. Brozio, A. Piehler, K.F. Renk, R. Berger, G. Saemann-Ischenko, Appl. Phys. Lett. 68 (1996) 1000.
[15] W. Assmann, J.A. Davies, G. Dollinger, J.S. Forster, H. Huber, Th. Reichelt, R. Siegele, Nuclear Instruments and Methods in Physics Research B 118 (1994) 242.
[16] M.P. Pechini, U.S. Patent No. 3,330,697 (1967).
[17] R. Mahesh, R. Nagarajan, C.N.R. Rao, Journal of Solid State Chemistry 96 (1992) 2.
[18] N. Klein, G. Müller, H. Piel, B. Roas, L. Schultz, U. Klein, M. Peiniger, Appl. Phys. Lett. 54 (1989) 757.
[19] G. Calestani, F.C. Matacotta, A. Migliori, P. Nozar, L. Roghi, K.A. Thomas, Physica C 261 (1996) 38.